Materials Research Bulletin 44 (2009) 1183–1187

Contents lists available at ScienceDirect

Materials Research Bulletin

journal homepage: www.elsevier.com/locate/matresbu

Short communication

The photoluminescence properties of Eu^{3+},Bi^{3+} co-doped yttrium oxysulfide phosphor under vacuum ultraviolet excitation

Zhilong Wang [a], Yuhua Wang [a], Jiachi Zhang [a,*], Yanghua Lu [b]

[a] Department of Materials Science, Lanzhou University, Lanzhou 730000, PR China
[b] Shenzhen Star Optoelectronic Technology Co., Ltd., Shenzhen 518100, PR China

ARTICLE INFO

Article history:
Received 23 May 2007
Received in revised form 4 November 2008
Accepted 5 November 2008
Available online 13 November 2008

Keywords:
A. Optical materials
D. Luminescence
D. Optical properties

ABSTRACT

Y_2O_2S co-doped with Bi^{3+},Eu^{3+} phosphors were prepared and their luminescence properties under vacuum ultraviolet (VUV) excitation were investigated. Much stronger red emission for Y_2O_2S:Eu^{3+},Bi^{3+} were observed under 147 nm excitation than that for Y_2O_2S:Eu^{3+}. Investigation on photoluminescence and calculation of electronic structure of Y_2O_2S:Eu^{3+},Bi^{3+} revealed that the Bi^{3+} acts as a medium in energy transfer process and the great VUV luminescence enhancement of Y_2O_2S:Eu^{3+} by doping Bi^{3+} is due to effective energy transfer process: charge transfer (CT) transition of Y^{3+}–$O^{2-} \rightarrow Bi^{3+} \rightarrow Eu^{3+}$. The Y_2O_2S:Eu^{3+},Bi^{3+} showed excellent optical properties when compared with the commercial (Y,Gd)BO_3:Eu^{3+}. Thus, the Y_2O_2S:Eu^{3+},Bi^{3+} would be a promising VUV-excited red phosphor.

1. Introduction

Recently, many researches have been focused on vacuum ultraviolet (VUV, 100–200 nm) excited phosphors because of the demands of the backlight of liquid crystal display (LCD) and Hg-free fluorescent lamp [1–3]. As the most important part of LCD backlight and Hg-free fluorescent lamp devices, VUV-excited phosphors require high brightness and pure color purity under 147 nm excitation [4]. Tricolor inorganic phosphors are used to emit red, green and blue light. (Y,Gd)BO_3:Eu^{3+} and Y_2O_3:Eu^{3+} are the main currently used commercial red VUV-excited phosphors. However, the dominant yellow emission at about 594 nm of (Y,Gd)BO_3:Eu^{3+} results in bad color purity which is not satisfying the requirement in display [5]. Y_2O_3:Eu^{3+} phosphor, despite its pure color purity, its brightness under 147 nm excitation is inadequate for need of lighting [6]. As a result, finding a suitable VUV-excited red phosphor which not only satisfies color purity but also has high photoluminescence intensity in VUV region becomes an emergency work.

Rare earth-doped oxysulfide Y_2O_2S has been utilized for efficient luminescent phosphors more than 30 years [7–10]. The crystal structure of Y_2O_2S belongs to hexagonal system and the Y atom is coordinated by four O atoms and three S atoms. Two Y atoms are μ-bridged by O and/or S atoms in the crystal so that the stability of Y_2O_2S is desirable when compared with other sulfide phosphor such as ZnS:Cu [11]. Eu^{3+}-doped Y_2O_2S red-emitting phosphor has been widely used in the field of color monitor tube (CMT) and high-resolution cathode ray tubes (CRTs) for its high luminous efficiency in UV region (254 nm) [7]. However, to the best of our knowledge, Y_2O_2S:Eu^{3+} has never been reported as a VUV-excited phosphor and its photoluminescence properties in VUV region has not been studied yet. In addition, as a full-developed phosphor, if Y_2O_2S:Eu^{3+} had strong absorption in VUV region, its application in LCD backlight and Hg-free lamp fields will be carried out quickly and easily. It is our basic aim to investigate the possibility of Y_2O_2S:Eu^{3+} to be used as a suitable VUV-excited red phosphor. On the other hand, it is known that the Bi^{3+} ion is a very good sensitizer of luminescence by strengthening and broadening UV–VUV excitation bands [12]. Thus, the incorporation of some Bi^{3+} ions may be favorable for the photoluminescence of Y_2O_2S:Eu^{3+} in VUV region. Based on these above reasons, in this work, the Eu^{3+} and Bi^{3+} co-doped Y_2O_2S phosphors were prepared by flux method. Their photoluminescence properties in VUV region and electronic structure were investigated in detail. The results showed that the Y_2O_2S:Eu^{3+},Bi^{3+} would be a very promising VUV-excited red phosphor applied in LCD backlight and Hg-free lamp.

2. Experimental and computational methodology

Y_2O_2S:Eu^{3+},Bi^{3+} powders were synthesized by flux method. The starting materials were Y_2O_3 (99.99%), Eu_2O_3 (99.99%), Bi_2O_3 (99.99%), S (≥99.5%). Stoichiometric amount of reagents were mixed homogeneously and fired at 1250 °C for 2 h in pure N_2 atmosphere. After the firing process, powders were washed with

* Corresponding author.
E-mail address: zhangjch03@lzu.cn (J. Zhang).

0025-5408/$ – see front matter © 2008 Elsevier Ltd. All rights reserved.
doi:10.1016/j.materresbull.2008.11.003

water to remove the residual flux and flux by-products and then etched with 5% HNO_3 solution for a clean, smooth particle surface. For comparison and discussion, the $Gd_2O_2S:Eu^{3+}$, $Y_2O_2S:Tb^{3+}$ phosphors were also prepared by the same method.

Rigaku D/Max-2400 X-ray diffractometer was employed to check the phase of the phosphor powder using Cu Kα radiation. The inductively coupled plasma (ICP) spectrometry data were taken with an IRIS Advantage ER/S ICP emission spectrometer instrument (U.S.A Termal Jarrell-Ash Corporation). The excitation and emission spectra were measured at room temperature using an Edinburgh Instruments FLS920T combined Fluorescence Lifetime and steady-state spectrophotometer with Xe900 (450 W xenon arc lamp) as excitation source. The light source of the VUV excitation part of the spectrometer system was a 150-W Deuterium lamp (Cathodeon Incorporated) and the emission and excitation spectra were measured by the vacuum monochromator (VM504, Acton Research Corporation, ARC). The VUV excitation spectra were corrected by dividing the excitation intensity of sodium salicylate under the same measurement conditions.

All the calculations are based on the local density approximation (LDA) of the density functional theory (DFT) [13,14]. CASTEP [15–17], used in the present work is based on planewaves and pseudopotentials. The considered valence electrons for Y, S and O are $4d^15s^2$, $3s^23p^4$ and $2s^22p^4$, respectively. The tested rather soft and optimized O pseudopotential in several systems [18–20] enable us to use a kinetic-energy cutoff of 460 eV throughout the calculation and its reliability will be further demonstrated in the results of the optical properties calculation.

3. Results and discussion

Fig. 1 shows the XRD patterns of Y_2O_2S (a), $Y_{1.96}Eu_{0.04}O_2S$ (b) and $Y_{1.94}Eu_{0.04}Bi_{0.02}O_2S$ (c) samples. As shown in Fig. 1, all oxysulfide samples in this work are well indexed to a hexagonal crystal structure with the space group $P3m1$ (No. 164) and are characterized as single phase based on JCPDF card number: 29-0351. The results also indicate that the small amount Eu^{3+} and Bi^{3+} ions doping do not change the basic crystal structure of Y_2S_2O phase. Generally, the Eu^{3+} and Bi^{3+} doped content in this work was very small (<3%), so it would be not very difficult for Eu^{3+} and Bi^{3+} to be doped into the Y_2O_2S lattices. The ICP experimental element analysis data in Table 1 further confirms that the formation of $Y_2O_2S:Eu^{3+},Bi^{3+}$ samples is accompanied by the incorporation of

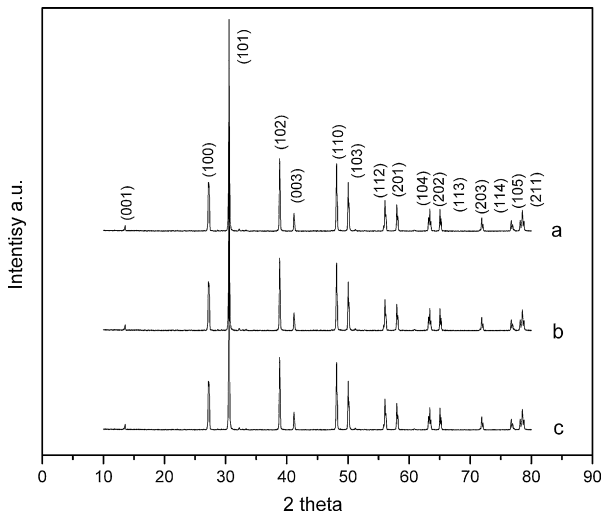

Fig. 1. XRD patterns of Y_2O_2S (a), $Y_{1.96}Eu_{0.04}O_2S$ (b) and $Y_{1.94}Eu_{0.04}Bi_{0.02}O_2S$ (c) samples.

Table 1
The ICP experimental element analysis data of $Y_{1.94}Eu_{0.04}Bi_{2x}O_2S$ ($0.01 \le x \le 0.03$).

Samples	ICP(%)		
	Y	Eu	Bi
$x = 0.1$	97.19	1.95	0.86
$x = 0.2$	96.25	1.92	1.83
$x = 0.3$	95.32	1.93	2.75

Bi^{3+} into the lattice. However, the Bi concentrations obtained by ICP were found to be still lower by the expected values and it could be explained as the unexpected lose of Bi^{3+} which stays apart as Bi_2O_3 or Bi_2S_3 and is dissolved later by HNO_3 in experimental process. And another proof of Bi^{3+} inclusion would be presented in the following photoluminescence parts.

As for typical samples, the emission spectra of the $Y_{1.96}Eu_{0.04}O_2S$ (a) and $Y_{1.94}Eu_{0.04}Bi_{0.02}O_2S$ (b) under 147 nm excitation are illustrated in Fig. 2. The inset in Fig. 2 exhibits the emission intensity of $^5D_0$–$^7F_2$ (626 nm) transition of Eu^{3+} in $Y_{2(1-x)}Eu_{2x}O_2S$ under 147 nm excitation dependent on Eu^{3+} doped concentration. It can be observed that the emission intensity gradually increases with increasing of Eu^{3+} concentration at first. When x is up to 0.02, the emission intensity reaches a maximum, and then decreases rapidly by increasing Eu^{3+} concentration, which is due to the concentration quenching effect. Based on this result, the Eu^{3+} doped concentration of all oxysulfide samples is fixed to 2% in the following work.

As shown in Fig. 2(a), it is observed that the emission spectrum of $Y_{1.96}Eu_{0.04}O_2S$ under 147 nm excitation consists of the four main emission lines: $^5D_0$–$^7F_1$ (587 nm), $^5D_0$–$^7F_2$ (626 nm), $^5D_0$–$^7F_4$ (685 nm) and $^5D_0$–$^7F_5$ (705 nm) transitions. Among them, the emission peak of electric-dipole $^5D_0$–$^7F_2$ transition of Eu^{3+} at about 626 nm is dominant while the magnetic-dipole $^5D_0$–$^7F_1$ transition is very weak. The results indicate that the Eu^{3+} ions in $Y_2O_2S:Eu^{3+}$ occupy the lattice sites without inversion symmetry. As a result, the VUV luminescence of $Y_2O_2S:Eu^{3+}$ phosphor exhibits better color purity when compared with that of the commercial $(Y,Gd)BO_3:Eu^{3+}$ phosphor in which the $^5D_0$–$^7F_1$ transition at 594 nm is as high as the $^5D_0$–$^7F_2$ transition at 612 nm [21]. As can be seen in Fig. 2(b), by doping of 1 mol% Bi^{3+} into the $Y_{1.96}Eu_{0.04}O_2S$, the emission intensity of $^5D_0$–$^7F_1$ transition of Eu^{3+}

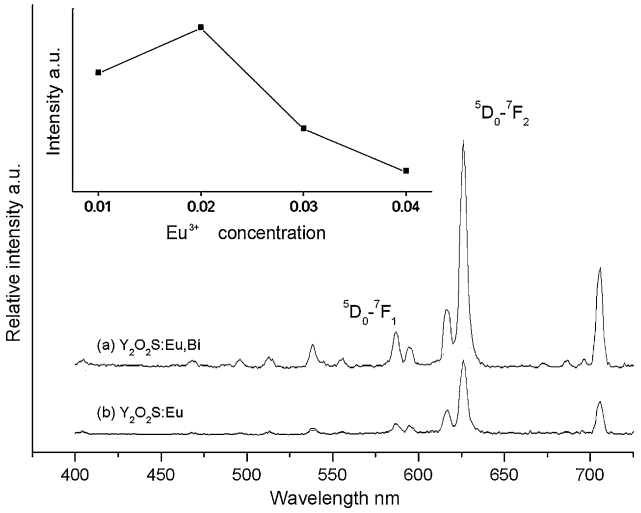

Fig. 2. The emission spectra of the $Y_{1.96}Eu_{0.04}O_2S$ (a) and $Y_{1.94}Eu_{0.04}Bi_{0.02}O_2S$ (b) samples under 147 nm excitation; inset shows the emission intensity of $^5D_0$–$^7F_1$ (626 nm) transition of Eu^{3+} in $Y_{2(1-x)}Eu_{2x}O_2S$ under 147 nm excitation dependent on Eu^{3+} doped concentration.

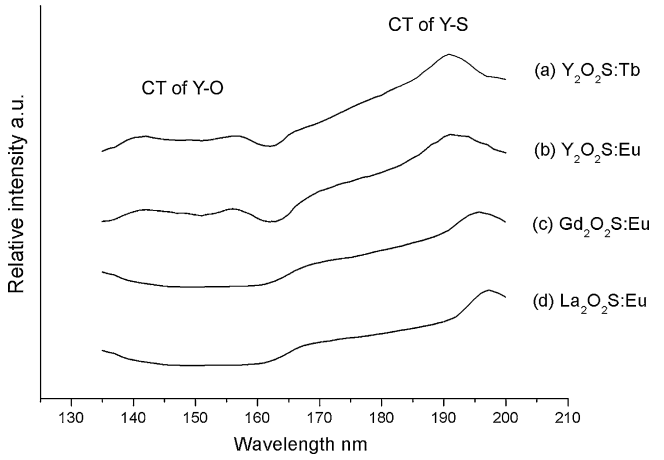

Fig. 3. The VUV excitation spectra in 135–200 nm of $Y_{1.98}Eu_{0.02}O_2S$ (a), $Y_{1.98}Tb_{0.02}O_2S$ (b), $Gd_{1.98}Eu_{0.02}O_2S$ (c) and $La_{1.98}Eu_{0.02}O_2S$ (d) sample.

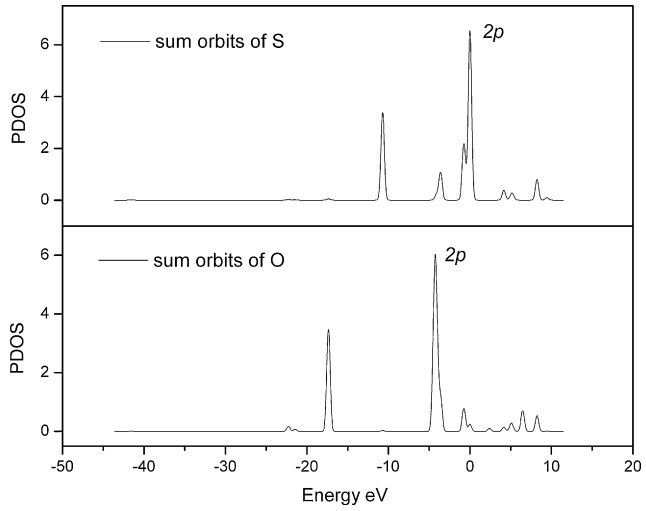

Fig. 4. The p orbital resolved partial density of states (PDOS) of O and S atom in Y_2O_2S crystal.

in $Y_{1.94}Eu_{0.04}Bi_{0.02}O_2S$ sample (b) is higher by 150% than that in $Y_{1.96}Eu_{0.04}O_2S$ sample (a). This result indicates that the doping of 1 mol% Bi^{3+} greatly improves the photoluminescence of $Y_2O_2S:Eu^{3+}$ phosphor under 147 nm excitation.

In order to explain the VUV-excited photoluminescence enhancement of $Y_2O_2S:Eu^{3+}$ by doping Bi^{3+}, their excitation spectra in VUV region should be identified at first. Fig. 3 illustrates the VUV excitation spectra in 135–200 nm of $Y_{1.98}Eu_{0.02}O_2S$ sample (a). For comparison, it gives those of $Y_{1.98}Tb_{0.02}O_2S$ (b), $Gd_{1.98}Eu_{0.02}O_2S$ (c) and $La_{1.98}Eu_{0.02}O_2S$ (d). In Fig. 3, we focus on two main excitation regions: the 141–163 nm band and band centered at 196 nm. Considering that the Y_2O_2S host absorption is located at about 262 nm in UV region [7–10], there two excitation bands may be assigned to be the transition of the electrons from the 2p state of ligand to the yttrium conduction band, viz. charge transfer (CT) band of Y^{3+}–O^{2-} or Y^{3+}–S^{2-} (1), as can be seen in spectra of yttrium-contained $Y_2O_2S:Eu^{3+}$ (a) and $Y_2O_2S:Tb^{3+}$ (b) samples, there is a particular excitation band with two small peaks in 141–163 nm. However, this excitation is not observed for $Gd_2O_2S:Eu^{3+}$ (c) and $La_2O_2S:Eu^{3+}$ (d). Therefore, the excitation in 141–163 nm should be correlated with yttrium. The 141–163 nm band could be attributed to the transition of the electrons from the oxygen 2p state to the yttrium conduction band, viz. CT of Y^{3+}–O^{2-} [22]. In addition, Table 2 gives the positions of Y^{3+}–O^{2-} CT transition in some other oxides which were identified experimentally. It can be seen that the CT transition of Y^{3+}–O^{2-} in many oxides are generally at around 150 nm. Therefore, it is reasonable to ascribe the excitation band of Y_2O_2S:Eu in 141–163 nm to the CT transition of Y^{3+}–O^{2-} (2), as for the broad excitation peaks centered at about 196 nm in excitation spectra of $Y_{1.98}Eu_{0.02}O_2S$ (a) and $Y_{1.98}Tb_{0.02}O_2S$ (b) samples, they could be assigned to CT transitions of Y^{3+}–S^{2-}. The similar excitation peaks centered at 200 nm in $Gd_2O_2S:Eu^{3+}$ sample (c) and at 205 nm in $La_2O_2S:Eu^{3+}$ (d) should be due to the CT transition of Gd^{3+}–S^{2-} and La^{3+}–S^{2-}, respectively. These results indicate that the VUV-excited photoluminescence of $Y_2O_2S:Eu^{3+}$ phosphors mainly derives from the CT transition of Y^{3+}–O^{2-} and Y^{3+}–S^{2-}. These above identification can be further confirmed by the electron structure calculation of Y_2O_2S crystal. Fig. 4 shows the p orbital resolved partial density of states of O and S atom in Y_2O_2S crystal. As shown in Fig. 4(a), the peak at −0.01 eV is due to the 2p orbit of S while the O-2p atomic orbital in the basis function is at a lower energy level in valence band (−4.25 eV). This result indicates that the CT energy of Y^{3+}–O^{2-} is higher than that of Y^{3+}–S^{2-} and it could be also explained by the smaller electronegative of S^{2-} than O^{2-}, which causes the CT transition of Y^{3+}–S^{2-} locating at a longer wavelength than that of Y^{3+}–O^{2-}.

After identifying these excitation bands of $Y_2O_2S:Eu^{3+}$ in UV–VUV region, the luminescence enhancement by doping Bi^{3+} could be revealed. Fig. 5 gives the VUV excitation spectra (135–200 nm) of $Y_{1.94}Eu_{0.04}Bi_{0.02}O_2S$ (a), $Y_{1.96}Eu_{0.04}O_2S$ (b) and $Y_{1.96}Bi_{0.04}O_2S$ (c) samples. As shown in Fig. 5(a), by doping 1 mol% Bi^{3+}, the CT transition of Y^{3+}–O^{2-} (141–163 nm) and the excitation region in the 175–187 nm region are obviously enhanced. By comparison of the excitation spectrum of $Y_{1.94}Eu_{0.04}Bi_{0.02}O_2S$ (a) with that of $Y_{1.96}Bi_{0.04}O_2S$ (c), it was found that the luminescence enhancement in 175–187 nm mainly derives from the absorption of characteristic $^1S_0$–$^1P_1$ transition of Bi^{3+}. This result indicates that, when

Table 2
The probable positions of charge transfer (CT) transition of Y^{3+}–O^{2-} in some other oxides.

Phosphors	CT position (λ_{max}, nm)	Ref.
$YPO_4:Tb^{3+},Ce^{3+},Pr^{3+}$	149	[23,24]
$YBO_3:Eu^{3+}$	149	[25]
$Y_4Al_2O_9:Eu^{3+}$	141	[26]
$YAlO_3:Eu^{3+}$	153	[27]
$(Gd,Y)BO_3:Tb^{3+}$	150	[28]

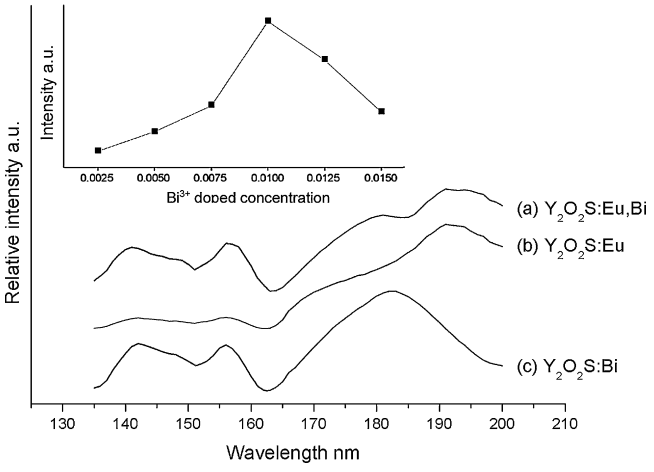

Fig. 5. The VUV excitation spectra in 135–200 nm of $Y_{1.94}Eu_{0.04}Bi_{0.02}O_2S$ (a), $Y_{1.96}Eu_{0.04}O_2S$ (b) and $Y_{1.96}Bi_{0.04}O_2S$ (c) samples. Inset shows the emission intensity of Bi^{3+} in $Y_{2(0.98-x)}Bi_xEu_{0.04}O_2S$ under 147 nm excitation dependent on Bi^{3+} doped concentration.

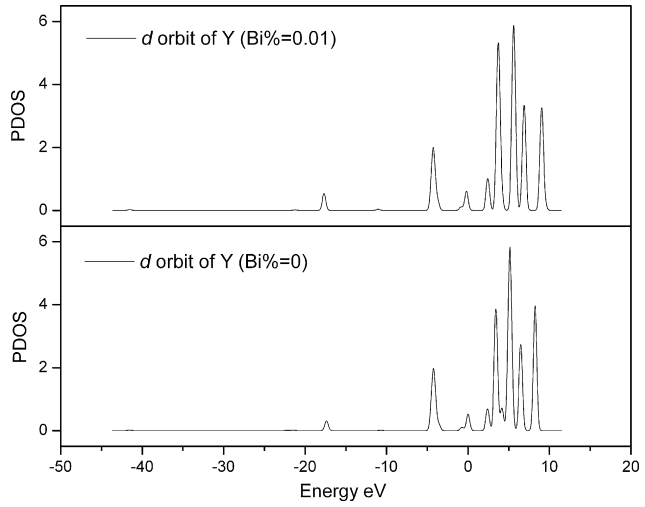

Fig. 6. The partial density of states (DOS) of Y-4d orbits.

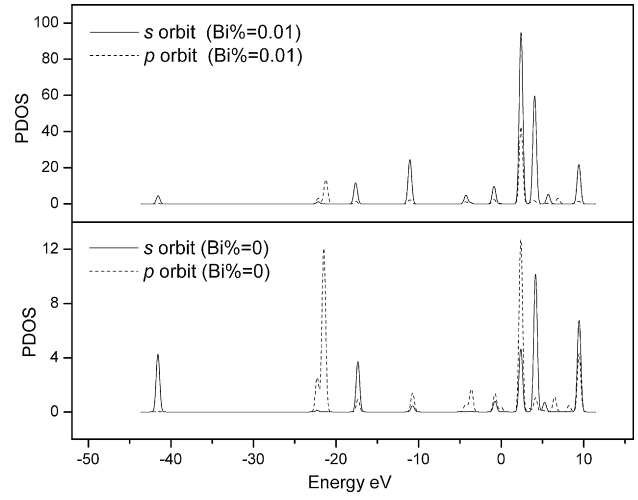

Fig. 7. The partial DOS of Y-s,p orbits.

excited by 175–187 nm, the excitation energy of Bi^{3+} is effectively transferred to Eu^{3+} for emission in $Y_2O_2S:Eu^{3+},Bi^{3+}$ system. On the other hand, it is very important to note that both CT transitions of Y^{3+}–O^{2-} in $Y_{1.94}Eu_{0.04}Bi_{0.02}O_2S$ (a) and $Y_{1.96}Bi_{0.04}O_2S$ (c) are very intense, but it is weak in $Y_{1.96}Eu_{0.04}O_2S$ (b). The results indicate that the direct energy transfer process from CT transition of Y^{3+}–O^{2-} to Eu^{3+} ions may be not efficient. But it becomes much easier through Bi^{3+} as a medium, viz. CT of Y^{3+}–$O^{2-} \rightarrow Bi^{3+} \rightarrow Eu^{3+}$.

As shown in the inset of Fig. 5, the concentration of Bi^{3+} should be carefully controlled for the best luminescence intensity under 147 nm excitation and the optimum Bi^{3+}-doped concentration is 1 mol%. It is understandable that the luminescence intensity of $Y_2O_2S:Eu^{3+}$ cannot be controlled and the optical characteristic transitions of Bi^{3+} cannot be observed if the Bi stays apart as Bi_2O_3 or Bi_2S_3, and it further confirms the Bi^{3+} inclusion in the lattice of Y_2O_2S.

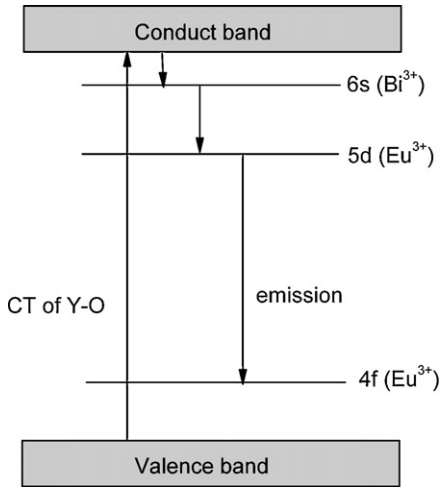

Fig. 8. A possible energy transfer scheme in $Y_2O_2S:Eu^{3+},Bi^{3+}$.

In order to further confirm the above observations and establish a scheme of the energy transfer pathway in $Y_2O_2S:Eu^{3+},Bi^{3+}$ system, the partial density of states (DOS) of Y were studied. Figs. 6 and 7 exhibit the partial DOS of Y-4d and Y-s,p orbits, respectively. It is found that, by doping 1 mol% Bi^{3+}, the DOS of Y-4d do not show obvious change and it indicates that the Y–O CT may be not affected by the doping of Bi^{3+} while the improvement of Y–O CT in Fig. 5 should mainly derive from the increase of energy transfer efficiency from Y–O CT to Bi^{3+}. Since the ground state of a free ion of Bi^{3+} is the $^1S_0$ state with a $6s^2$ configuration, the sharp increase of the DOS of sp component should be due to the small amount doping of Bi^{3+} ions and it could confirm the generation of strong S_0–$^1P_1$ absorption of Bi^{3+}. Considering that the valence electrons of Bi^{3+} $6s^2$ configuration is located at a lower energy than that of the Y-4d, it is understandable that the energy transfer pathway is Y^{3+}–$O^{2-} \rightarrow Bi^{3+} \rightarrow Eu^{3+}$, and the Bi^{3+} acts as a medium in energy transfer process. Based on the above results, a possible energy transfer scheme is proposed in Fig. 8.

Table 3 exhibits the comparison of main optical properties of $Y_2O_2S:Eu^{3+}$, $Y_2O_2S:Eu^{3+},Bi^{3+}$ and the commercial $(Y,Gd)BO_3:Eu^{3+}$ phosphor. The main data of optical properties were calculated by "Zolix Color Convert" program from their VUV-excited photoluminescence spectra. The brightness of phosphors was measured by "Photon PR880" VUV spectrophotometer. It is found that this $Y_2O_2S:Eu^{3+},Bi^{3+}$ phosphor shows good emission purity and comparable brightness when compared with the commercial $(Y,Gd)BO_3:Eu^{3+}$ phosphor. Significantly, the chromaticity of $Y_2O_2S:Eu^{3+},Bi^{3+}$ is more close to commercial standard and it means a improvement of color purity for displays or lamps. Therefore, it can be concluded that this $Y_2O_2S:Eu^{3+},Bi^{3+}$ phosphor is a very promising VUV-excited red candidate for application in LCD backlight and Hg-free fluorescent lamps.

Table 3
The comparison of main optical properties of $Y_2O_2S:Eu^{3+}$, $Y_2O_2S:Eu^{3+},Bi^{3+}$ and commercial $(Y,Gd)BO_3:Eu^{3+}$ phosphor.

	$Y_2O_2S:Eu$	$Y_2O_2S:Eu,Bi$	$(Y,Gd)BO_3:Eu$	Commercial standard [29]
Purity of emission	0.71	0.89	0.75	1
Half breadth of emission	3.32	3.10	4.58	Narrow
Characteristic red emission	626 nm	626 nm	612 nm	–
Chromaticity coordinations	(0.636, 0.321)	(0.640, 0.324)	(0.60, 0.334)	(0.67, 0.33)
Relative integral brightness	60	96	100	–

4. Conclusions

The photoluminescence of $Y_2O_2S:Eu^{3+},Bi^{3+}$ red phosphor under 147 nm excitation were enhanced significantly by additional doping of Bi^{3+} ions. The study on VUV-excited photoluminescence spectra and electronic structure revealed that the Bi^{3+} acts as an effective medium in energy transfer process, viz. CT of Y^{3+}–$O^{2-} \rightarrow Bi^{3+} \rightarrow Eu^{3+}$. The comparison between $Y_2O_2S:Eu^{3+},Bi^{3+}$ and the commercial $(Y,Gd)BO_3:Eu^{3+}$ phosphor shows that $Y_2O_2S:Eu^{3+},Bi^{3+}$ is a very promising VUV-excited red phosphor applied in LCD backlight and Hg-free fluorescent lamps.

Acknowledgements

This work was supported by Program for New Century Excellent Talents in University of China (NCET, 04-0978) and Chinese Specialized Research Fund for the Doctoral Program of Higher Education (SRFDP, 20040730019).

References

[1] T. Shinoda, ASID'04 Proceedings of the 8th Asian Symposium on Information Display, vol. 1, 2004.
[2] C. Okazaki, M. Shiiki, T. Suzuki, K. Suzuki, J. Lumin. 87–89 (2000) 1280.
[3] T. Justel, J.-C. Krupa, D.U. Wiechert, J. Lumin. 93 (2001) 179.
[4] X.-N. Liu, H.-B. Cui, Y. Tang, S.-X. Huang, W.-H. Liu, C. Gao, Appl. Surf. Sci. 223 (2004) 144.
[5] L. Tian, B.Y. Yu, C.H. Pyun, H.L. Park, S. Mho, Solid. State. Commun. 129 (2004) 43.
[6] C.H. Kim, I.E. Kwon, C.H. Park, Y.J. Hwang, H.S. Bae, B.Y. Yu, C.H. Pyun, G.Y. Hong, J. Alloy Compd. 311 (2000) 33.
[7] P.N. Yocom, U.S. Patent, 3,418,247 (1968).
[8] H. Yamamoto, J. Electrochem. Soc. 126 (1979) 305.
[9] M. Pham-Thi, J. Electrochem. Soc. 138 (1991) 1100.
[10] Y. Kawahara, Chem. Mater. 18 (2006) 6303.
[11] Toshie Harazono, Ryuji Adachi Shimomura, J. Phys. Chem. 3 (2001) 2943.
[12] S. Neeraj, N. Kijima, A.K. Cheetham, Solid. State. Commun. 131 (2004) 65–69.
[13] P. Hohenberg, W. Kohn, Phys. Rev. 136 (1964) B864.
[14] W. Kohn, L.J. Sham, Phys. Rev. 140 (1965) A1133.
[15] CASTEP 3.5 program developed by Molecular Simulations Inc., 1997.
[16] M.C. Payne, M.P. Teter, D.C. Allan, T.A. Arias, J.D. Joannopoulos, Rev. Mod. Phys. 64 (1992 1045).
[17] M.D. Segall, P.J.D. Lindan, M.J. Probert, C.J. Pickard, P.J. Hasnip, S.J. Clark, M.C. Payne, J. Phys.: Condens. Matter. 14 (2002 2717).
[18] A. Takada, C.R.A. Catlow, J.S. Lin, G.D. Price, M.H. Lee, V. Milman, M.C. Payne, Phys. Rev. B 51 (1995) 1447.
[19] I. Dawson, P.D. Bristowe, M.H. Lee, M.C. Payne, M.D. Segall, J.A. White, Phys. Rev. B 54 (1996) 13727.
[20] M.H. Lee, C.F. Cheng, V. Heine, J. Klinowski, Chem. Phys. Lett. 265 (1997) 673.
[21] X.-C. Jiang, C.-H. Yan, L.-D. Sun, Z.-G. Wei, C.-S. Liao, J. Solid State Chem. 175 (2003) 245.
[22] T. Tomili, J. Tamashiro, Y. Tananara, et al. J. Phys. Soc. Jpn. 55 (1986) 4543.
[23] K.S. Sohn, Y.Y. Choi, H.D. Park, Y.G. Choi, J. Electrochem. Soc. 147 (2000) 2375.
[24] T.J. ustel, P. Huppertz, W. Mayr, D.U. Wiechert, J. Lumin. 106 (2004) 225.
[25] Y. Wang, X. Guo, T. Endo, Y. Murakami, M. Ushirozawa, J. Solid State Chem. 177 (2004) 2242.
[26] D.Y. Wang, Y.H. Wang, J. Alloy Compd. 425 (2006) L5.
[27] V.N. Abramov, A.I. Kuznetsov, Sov. Phys. Solid State 20 (1978) 399.
[28] Y. Wang, C. Wu, J. Zhang, Mater. Res. Bull. 41 (8) (2006) 1571.
[29] Y. Wang, J. Zhang, X. Guo, Electrochem. Solid-State. Lett. 9 (2006) H26.